responses in secondary dengue virus infections: levels and positive rates in comparison with primary infections. J Clin Virol 31:185–189

8. Sa-ngasang A, Anantapreecha S, A-nuegoonpipat A, Chanama S, Wibulwattanakij S, Pattanakul K, Sawanpanyalert P, Kurane I (2006) Specific IgM and IgG responses in primary and secondary dengue virus infections determined by enzyme-linked immunosorbent assay. Epidemiol Infect 134:820–825
9. Kochel TJ, Watts DM, Gozalo AS, Ewing DF, Porter KR, Russel KL (2005) Cross-serotype neutralization of dengue virus in *Aotus nancymae* monkeys. J Infect Dis 191:1000–1004
10. Endy TP, Nisalak A, Chunsuttitwat S, Vaughn DW, Green S, Ennis EA, Rothman A, Libraty D (2004) Relationship of preexisting dengue virus (DV) neutralizing antibody levels to viremia and severity of disease in a prospective cohort of DV infection in Thailand. J infect Dis 189:990–1000

Immunogenetics (2011) 63:501–509
DOI 10.1007/s00251-011-0531-y

ORIGINAL PAPER

ULBP4/RAET1E is highly polymorphic in the Old World monkey

Taeko K. Naruse · Yukiko Okuda · Kazuyasu Mori · Hirofumi Akari · Tetsuro Matano · Akinori Kimura

Received: 22 February 2011 / Accepted: 21 April 2011 / Published online: 7 May 2011

Abstract Natural-killer group 2 member D (NKG2D) is an activating receptor that plays an important role in the immune response mediated by NK cells, $\gamma\delta^+$ T cells, and $CD8^+$ T cells. In humans, MHC class I chain-related genes and UL-16 binding protein (ULBP)/retinoic acid early transcript 1 (REAT1) gene family encode ligands for NKG2D. The rhesus and crab-eating macaques, which belong to the Old World monkeys, are widely used as non-human primate models in medical researches on the immunological process. In the present study, we investigated the polymorphisms of *ULBP4/RAET1E*, a member of the *ULBP/RAET1* family, and found 25 and 14 alleles from the rhesus and crab-eating macaques, respectively, of which diversities were far more extended than in humans. A phylogenetic study suggested that the allelic diversification of ULBP4/RAET1E predated the divergence of rhesus and crab-eating macaques.

T. K. Naruse · A. Kimura (✉)
Department of Molecular Pathogenesis, Medical Research Institute, Tokyo Medical and Dental University,
1-5-45 Yushima, Bunkyo-ku,
Tokyo 113–8510, Japan
e-mail: akitis@mri.tmd.ac.jp

Y. Okuda · A. Kimura
Laboratory of Genome Diversity, Graduate School of Biomedical Science, Tokyo Medical and Dental University,
Tokyo, Japan

K. Mori · T. Matano
AIDS Research Center, National Institute of Infectious Diseases,
Tokyo, Japan

H. Akari
Primate Research Institute, Kyoto University,
Inuyama, Japan

T. Matano
International Research Center for Infectious Diseases,
The Institute of Medical Science, The University of Tokyo,
Tokyo, Japan

Keywords Rhesus macaque · Crab-eating macaque · ULBP4/RAET1E · NKG2D · Polymorphism

Introduction

Non-human primates, such as rhesus and crab-eating macaques, are important animal models for the study of infectious diseases, autoimmune diseases, and organ transplantation. These macaques are members of the Old World monkeys, and it has been reported that the genetic diversity in the rhesus macaque is quite unique, that is, more than 60% of the rhesus macaque-specific expansions are found in the protein coding sequences (Gibbs et al. 2007). To evaluate the results of immunological experiments in the macaque models, it is essential to characterize the genetic diversity of immune-related molecules which may control the individual differences in the immune response against foreign antigens and/or pathogens. It has been reported that the gene copy number in the major histocompatibility complex (MHC) loci in the rhesus and crab-eating macaques is higher than that in humans (Kulski et al. 2004; Gibbs et al. 2007; Otting et al. 2007). In addition, the extent of genetic diversity differed, in part, depending on the geographic areas, and we have reported that the diversity of MHC class I genes in the rhesus macaque is considerably different depending on habitat (Naruse et al. 2010).

Because the innate immune system is involved in the response to environmental pathogens, it is necessary to consider the function of natural killer (NK) cells in the experimental animal models. Natural-killer group 2 member D (NKG2D), a C-type lectin molecule, is an activating receptor expressed on the cell surface of NK, $\gamma\delta^+$, and $CD8^+$ T cells, which plays an important role in the immune response (Wu et al. 1999; Raulet 2003). In humans, MHC class I chain-related genes (MIC) and UL-16 binding protein (ULBP)/retinoic acid early transcript 1 (REAT1)

gene family are known to encode ligands for NKG2D (Bauer et al. 1999; Cosman et al. 2001; Chalupny et al. 2003; Bacon et al. 2004). These ligand molecules are usually stress-inducible, and their recognition by NKG2D can lead to the activation of NK cells, consequently killing virus-infected and tumor cells (Pende et al. 2002; Eagle et al. 2006; Pappworth et al. 2007; Ward et al. 2007).

The human *ULBP/RAET1* gene family is located on chromosome 6q24.2, which is composed of ten members including six functional genes, *ULBP1*, *2*, *3*, *4*, *5*, and *6*, corresponding to *RAET1I*, *H*, *N*, *E*, *G*, and *L*, respectively (Radosavljevic et al. 2001; Chalupny et al. 2003; Eagle et al. 2009a, b). In addition, several sequence polymorphisms in each *ULBP* gene have been identified (Romphruk et al. 2009; Antoun et al. 2010). Although it is evident that the cell surface expression of the ligand molecules on target cells is differentially regulated (Eagle et al. 2006), genetic polymorphisms in the coding regions might have a functional impact. We have previously investigated the genetic polymorphisms of *ULBP/RAET1* genes and have found that the *ULBP4/RAET1E* gene is the most polymorphic, with the allelic distribution differing among ethnic groups (Romphruk et al. 2009).

On the other hand, rhesus macaque *ULBP4/RAET1E* (GenBank: NW_001116520) is mapped on the long arm of chromosome 4 (i.e., positions from 31, 164, 822 to 31, 175, 032 of chromosome 4 in the rhesus genome; data obtained from the UCSC Genome Browser at http://genome.ucsc.edu/cgi-bin/hgGateway; Gibbs et al. 2007). However, its genetic polymorphisms are poorly characterized, although the MIC gene polymorphisms are well studied in the rhesus macaque (Seo et al. 1999, 2001; Doxiadis et al. 2007; Averdam et al. 2007). In the present study, we investigated the polymorphisms of *ULBP4/RAET1E* in rhesus and crab-eating macaques. This is the first report demonstrating the extreme diversity of the NKG2D ligand in the Old World monkey.

Materials and methods

Animals

A total of 38 rhesus macaques from seven lineages previously analyzed for the MHC polymorphisms (Naruse et al. 2010) and 24 crab-eating macaques from five lineages were the subjects. They were maintained in the breeding colonies in Japan. The founders of the rhesus macaque colonies were captured in Myanmar and Laos, whereas the founders of crab-eating macaque colonies were captured in Indonesia, Malaysia, and the Philippines. All care, including blood sampling of animals, were in accordance with the guidelines for the Care and Use of Laboratory Animals published by the National Institutes of Health (NIH publication 85–23, revised 1985) and were subjected to prior approval by the local animal protection authority.

DNA extraction and sequencing analysis

Genomic DNAs from B lymphoblastoid cell lines of the rhesus macaque (Naruse et al. 2010) and from whole blood sample of the crab-eating macaque were extracted by using the QuickGene DNA kit (Fujifilm, Tokyo, Japan) according to the manufacturer's instructions. The genomic gene for *ULBP4/RAET1E* of rhesus and crab-eating macaques was amplified by polymerase chain reaction (PCR) with a primer pair designed for the region spanning from introns 1 to 3 of the rhesus gene (NC007861), ULBP4F (5′-TGGGCCTCTTCCCCTGTCC) and ULBP4R (5′-GTGGGAGGTGGGATGGG), using FastStart Taq DNA polymerase (Roche, Mannheim, Germany). The PCR condition was composed of the following steps: denaturation at 95°C for 4 min; 30 cycles of 95°C for 30 s, 63°C for 30 s, and 72°C for 45 s; and additional extension at 72°C for 7 min. The PCR products of about 1,200 bp in length were cloned into pSTBlue-1 AccepTer vector (Novagen, WI, USA) according to the manufacturer's instructions and were transformed to Nova Blue Single™ competent cells (Merck4Biosciences Japan, Tokyo, Japan). Ten to 20 independent transformant colonies were picked up for each sample and subjected to sequencing on both strands by using a BigDye Terminator cycling system and an ABI 3730 automated sequence analyzer (Applied Biosystems, CA, USA).

Data analyses

Nucleotide sequences of *ULBP4/RAET1E* from cloned DNAs were aligned using the Genetyx software package (version 8.0, Genetyx Corp., Japan). If at least three clones from independent PCR or from different individuals showed identical sequences, the sequences were submitted to the DNA Data Bank of Japan (DDBJ). Neighbor-joining trees were constructed with Kimura's 2-parameter method for a phylogenetic analysis of *ULBP4/RAET1E* sequences spanning from exons 2 to 3 including intron 2 by using the Genetyx software. Bootstrap values were based on 5,000 replications. The *ULBP4/RAET1E* sequences from humans (GenBank accession number AY252119), chimpanzees (AY032638), and rhesus (NC007861) were included in the analysis as references.

Structure model analysis

A three-dimensional (3-D) structure model of rhesus ULBP4/RAET1E, with amino acid positions from 1 to 178, was created by a molecular visualization software RasTop2.2 (http://sourceforge.net/projects/rastop/), and the

human RAET1B in complex with NKG2D (Radaev et al. 2001) from the Molecular Modeling Database (MMCB No. 18231) was used as the reference. Polymorphic sites were mapped on the 3-D structure model of macaque RAET1E by using the Cn3D 4.1 program (http://www.ncbi.nlm.nih.gov/Structure/CN3D/cn3d.shtml).

Table 1 Identified alleles of the ULBP4 gene in rhesus and cynomolgus

Species	Allele name	Accession no.	Reference animal	Identical sequence
Rhesus macaque	*Mamu-ULBP4*1.1*	AB568525	R228, R367	
	*Mamu-ULBP4*1.2*	AB568533	R492, R396, R465	
	*Mamu-ULBP4*2*	AB568526	R283, R384, R328, R337	
	*Mamu-ULBP4*3*	AB568527	R346, R361, R396, R379, R408	
	*Mmau-ULBP4*4*	AB568528	R320, R490, R321, R465, R367, R446, R328, R234, R237, R314	
	*Mamu-ULBP4*5*	AB568529	R430, R453, R325, R477, R439, R360, R379, R446, R355	
	*Mamu-ULBP4*6*	AB568530	R437, R350,	
	*Mamu-ULBP4*7.1*	AB568531	R325, R384, R491, R333, R337	
	*Mamu-ULBP4*7.2*	AB568544	R477	
	*Mamu-ULBP4*8*	AB568532	R408, R454, R241, R342, R316	
	*Mamu-ULBP4*9.1*	AB568534	R312, R314	
	*Mamu-ULBP4*9.2*	AB568535	R333	
	*Mamu-ULBP4*10*	AB568536	R316	
	*Mamu-ULBP4*11*	AB568537	R241	
	*Mamu-ULBP4*12*	AB568538	R342	
	*Mamu-ULBP4*13*	AB568539	R491	
	*Mamu-ULBP4*14*	AB568540	R495	*Mafa-ULBP4*1.1*
	*Mamu-ULBP4*15*	AB568541	R350	
	*Mamu-ULBP4*16*	AB568542	R492	
	*Mamu-ULBP4*17*	AB568543	R495	
	*Mamu-ULBP4*18*	AB568545	R454	
	*Mamu-ULBP4*19*	AB568546	R321	
	*Mamu-ULBP4*20*	AB568547	R355	
	*Mamu-ULBP4*21*	AB571025	R437	
	*Mamu-ULBP4*22*	AB571026	R439	
Crab-eating macaque	*Mafa-ULBP4*1.1*	AB578934	M01, P01, P02, C001, C003, C004, C005, C006	*Mamu-ULBP4*14*
	*Mafa-ULBP4*1.2*	AB578935	M02, C004	
	*Mafa-ULBP4*2*	AB578936	P04, M06, C010, C011, C013	
	*Mafa-ULBP4*3*	AB578938	M03, C007	
	*Mafa-ULBP4*4*	AB578939	M03, C006	
	*Mafa-ULBP4*5*	AB578940	P04, P05, M05, M06, C012, C013	
	*Mafa-ULBP4*6*	AB578941	M05, C010, C011	
	*Mafa-ULBP4*7.1*	AB578942	M01, C002	
	*Mafa-ULBP4*7.2*	AB578943	P03, C008	
	*Mafa-ULBP4*8*	AB578944	P03, M04, C008, C009	
	*Mafa-ULBP4*9*	AB578945	P01, C001, C002	
	*Mafa-ULBP4*10*	AB578946	M04, C009	
	*Mafa-ULBP4*11*	AB578947	P02, C007	
	*Mafa-ULBP4*12*	AB578948	M02, C005	

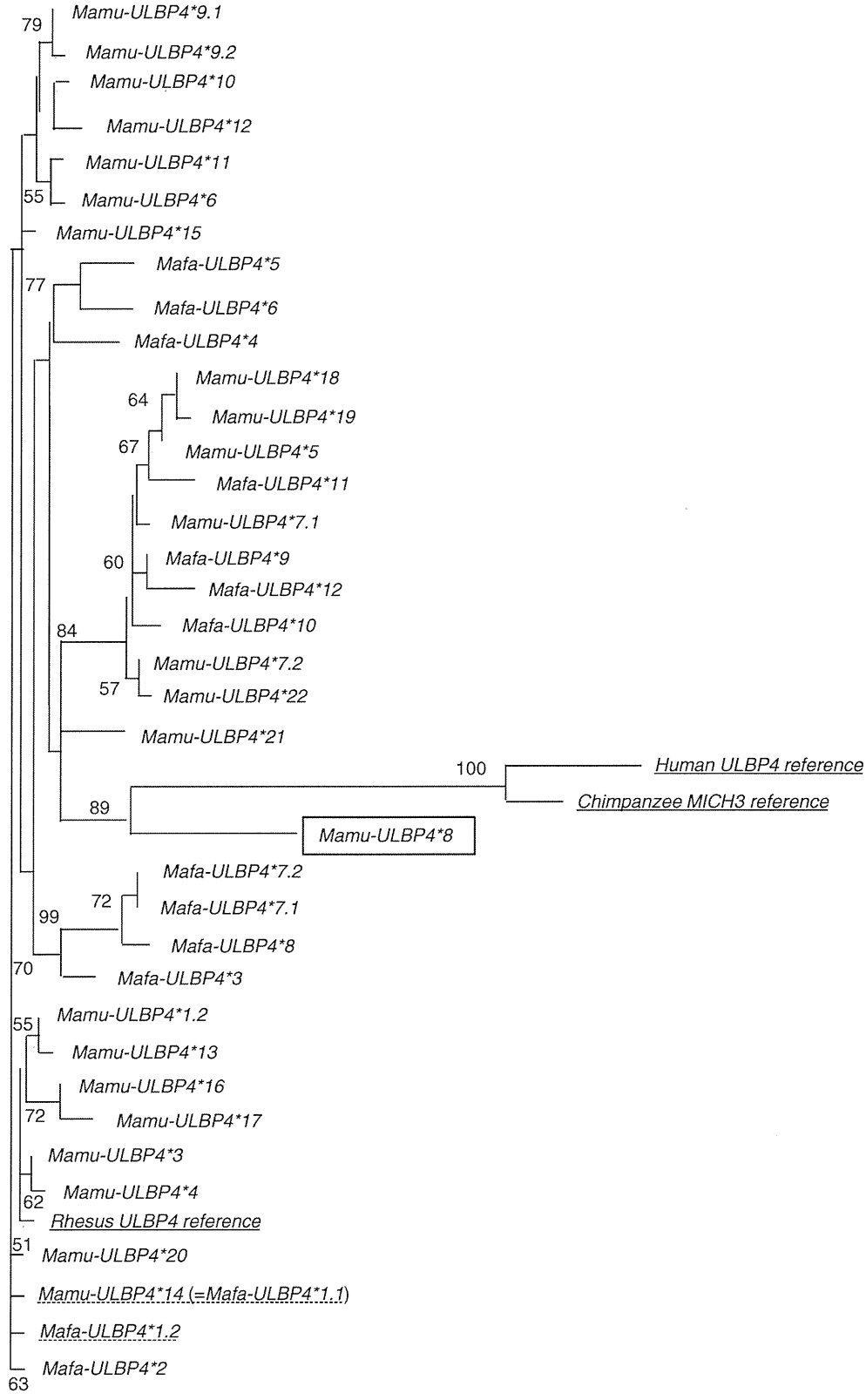

Fig. 1 Phylogenetic tree of *Mamu-* and *Mafa-ULBP4/RAET1E* alleles. A phylogenetic tree of *ULBP4/RAET1E* sequences spanning from exons 2 to 3, obtained in this study, was constructed by using the neighbor-joining method with bootstrap values of 5,000 replications. Values are indicated as percentages, and only those with more than 50% are shown. Sequences of human *ULBP4/RAET1E* (AY252119), chimpanzee *MICH3* (AY032638), and rhesus *ULBP4/RAET1E* (NC007861) were *underlined* and included in the analysis as reference sequences. Alleles represented with *broken underlines* had identical amino acid sequences predicted from the nucleotide sequences. The allele containing an in-frame termination codon was *boxed*

Results

ULBP4/RAET1E polymorphisms in the rhesus macaque

In the rhesus macaque genome (Gibbs et al. 2007), there are two paralogous genes for *ULBP4/RAET1E*, one of which appears to be functional, whereas the other is a pseudogene because it contains a large deletion containing the most part of exons 2, 3, and 4. Therefore, we designed primer pairs to amplify the region containing exons 2 and 3, which encode for α1 and α2 domains of ULBP4/RAET1E molecule, respectively, from the functional *ULBP4/RAET1E*. By using the primer pair, we obtained *ULBP4/RAET1E* sequences from 38 individuals of rhesus macaque. Because one or two sequences were obtained from each individual, the sequences were considered to be alleles of *ULBP4/RAET1E*. They were classified into 25 different alleles, designated as *Mamu-ULBP4*1.1* to *Mamu-ULBP4*22*, submitted to DDBJ, and given accession numbers (Table 1). The allele names with different numbers indicate that they are different in predicted amino acid sequences, whereas the alleles with the same deduced amino acid sequences but different nucleotide sequences, such as *Mamu-ULBP4*1.1* and *Mamu-ULBP4*1.2*, are designated as subtypes. None of the sequences obtained in this study was identical to the reference sequence, NC007861, which was previously deposited to the GenBank database as the rhesus *ULBP4/RAET1E*. On the other hand, when the sequences were aligned referring the human *ULBP4/RAET1E*, one rhesus allele (*Mamu-ULBP4*8*) was found to contain a nonsense mutation at codon 29, which would make the ULBP4/RAET1E molecule non-functional.

ULBP4/RAET1E polymorphisms in the crab-eating macaque

By using the primer pair designed for the rhesus *ULBP4/RAET1E*, we could amplify the *ULBP4/RAET1E* sequences from 24 individuals of the crab-eating macaque. Sequencing analysis revealed 14 different *ULBP4/RAET1E* alleles, and inheritance of each allele was confirmed by family studies. The identified allele sequences were submitted to DDBJ, given accession numbers, and designated as *Mafa-ULBP4*1.1* to *Mafa-ULBP4*12* (Table 1). The nucleotide sequences from exons 2 to 3 of *Mamu-ULBP4*14* were identical to those of *Mafa-ULBP4*1.1* and differed by only one nucleotide in intron 2 from those of *Mafa-ULBP4*1.2*. In addition, a neighbor-joining analysis performed by using nucleotide sequences spanning from exons 2 to 3 showed that the alleles of rhesus and crab-eating macaques were not separately clustered from each other (Fig. 1).

Comparative analysis of *ULBP4/RAET1E*

The alignment of *ULBP4/RAET1E* sequences from rhesus and crab-eating macaques with those from humans and chimpanzees showed that the macaque genes were homologous to the human gene by more than 90% and were equally diverged (Fig. 2). In addition, rhesus and crab-

```
                                                                    50
                Human :GHSLCFNFTI KSLSRPGQPW CEAQVFLNKN LFLQYNSDNN MVKPLGLLGK KVYATSTwge
           Chimpanzee :---------- -L-------- ---------- ---------- ---------- --N-------
        Rhesus macaque :A--------- --W------- ------M-K- -----D—S- ---------- --N-----Q-
  Crab-eating macaque :A--------- --W------- ------M--- -F---D—SN ---------- --N-----Q-

                                                          100
                Human :ltqtlgevgr dlrmllcdIK PQIKTSDPST LQVEMFCQRE AERCTGASWQ FATNGEKSLL
           Chimpanzee :---M------ ------L--- ------G--- ---------- ---------- --I-------
        Rhesus macaque :---K------ ------L-V- ------GP-- -----L---- ---------- -TI----C--
  Crab-eating macaque :---------- -LM---L-V- P-----G--- L----L---- ---------- -TI----C--

                                                  150
                Human :FDAMNMTWTV INHEAskike twkkdrglek yfrklskgdc dhwlreflgh weampEPTV
           Chimpanzee :---------- ---------- ---------- ---------- ---------- --------Q
        Rhesus macaque :F----M---- ----AS------ ---K------ ------M--- N------L-- Q-A-----Q
  Crab-eating macaque :---------- -----S---- ---------- ------M--- N-WLR----- Q------TQ
```

Fig. 2 Alignment of deduced amino acid sequences of α1 and α2 domains of ULBP4/RAET1E. Amino acid sequences were deduced from the nucleotide sequences of *ULBP4/RAET1E* or *MICH3* from humans (AY252119), chimpanzees (AY032638), rhesus macaques (NC007861), and crab-eating macaques (AY032639). *Numbers* above the sequences represent the amino acid positions in mature protein. *Dashes* indicate identical sequences. Sequences for the predicted α helix structure were indicated by *small italicized characters*. Positions of polymorphic sites in the *human*, *rhesus macaque*, and *crab-eating macaque* were *underlined*

Table 2 Single nucleotide polymorphisms of ULBP4 gene among human and Old World monkeys

	Number of alleles	Exon 2		Intron 2	Exon 3	
		Polymorphism	Non-synonymous change (%)	Polymorphism	Polymorphism	Non-synonymous change (%)
Human	5	2	2 (100%)	3	3	3 (100%)
Rhesus macaque	25	9	5 (55.6%)	22	22	14 (63.6%)
Crab-eating macaque	14	17	9 (52.9%)	18	16	9 (56.3%)

eating macaques showed a higher degree of polymorphism in the analyzed region, namely, exon 2, intron 2, and exon 3, than in humans (Table 2). All polymorphisms found in exons of human *ULBP4/RAET1E* were non-synonymous, whereas a considerable part of the polymorphisms were synonymous in the Old World monkeys. On the other hand, the polymorphic sites in the rhesus macaque (positions 29, 46, 59, 64, 79, 88, 112, 121, 126, 135, 136, 144, 157, 158, 161, 168, 171, and 173) and the crab-eating macaque (positions 32, 39, 40, 59, 72, 73, 79, 91, 112, 136, 163, 164, 165, 171, 178, and 179) were shared at five positions (59, 79, 112, 136, and 171) by each other, whereas only one position (position 112) was shared with polymorphic sites in humans (positions 53, 99, 112, and 113) (Fig. 2). In addition, a termination at position 29 was found in a rhesus macaque allele *Mamu-ULBP4*8*; a single amino acid deletion caused by deletions of a total of three nucleotides was found in a crab-eating macaque allele *Mafa-ULBP4*6* [i.e., TGGCTCAGG sequences corresponding to codons 163–165 were changed to TGCTCA, which may be due to two different deletions at codons 163 (from TGG to TG) and 165 (from AGG to A)], whereas such polymorphisms were not observed in humans. These findings suggest that a selection pressure to generate and maintain the polymorphic sites might be considerably different between the lineages of humans and the Old World monkeys.

Discussion

It has been suggested that the ancestral gene for the ULBP/REAT molecule of placental mammals was originally diverged and duplicated in each species after an emigration from the MHC region (Kondo et al. 2010). In humans, MHC genes (*HLA* genes) are clustered and mapped on the short arm of chromosome 6, 6p21.3, whereas the *ULBP/RAET1* genes are located on the long arm of chromosome 6, 6q25.1. As for the *MHC* genes in the macaque, it was previously reported that rhesus macaque MHC, e.g., BAT1 gene, was localized to chromosome 6q24 by using fiber-fluorescence in situ hybridization (Huber et al. 2003) and cynomolgus (crab-eating) macaque MHC, e.g., Mafa-A and Mafa-B genes, was cytogenetically mapped to chromosome 6p13 (Liu et al. 2007), although the rhesus macaque MHC is mapped on the short arm of chromosome 4 in the draft genome sequence database of rhesus macaques (Gibbs et al. 2007); e.g., Mamu-A and BAT1 were mapped from positions 29, 517, 308 to 29, 520, 221 and from 31, 164, 822 to 31, 175, 032, respectively, on chromosome 4 (data were obtained from the UCSC Genome Browser at http://genome.ucsc.edu/cgi-bin/hgGateway). The discrepancy between the cytogenetic mapping and the assignment in draft genome sequence should be resolved in the future. On the other hand, it is interesting to note that each member of the *ULBP/RAET1* gene family, except for *ULBP6*, is completely or partially duplicated in the rhesus genome. As for the *ULBP4/RAET1E*, two related sequences, LOC695031 (NC007861) and LOC694265, have been identified as orthologs of human *ULBP4/RAET1E*. On the other hand, the configuration of *ULBP/RAET1* loci in the crab-eating macaque genome remained unknown. Because LOC694265 was a pseudogene lacking most part of the coding exons, we designed PCR primers by referring the NC007861 sequence. By using the designed primers, we could successfully amplify *ULBP4/RAET1E* alleles from both rhesus and crab-eating macaques.

In this study, we identified a total of 25 and 14 alleles from rhesus and crab-eating macaques, respectively. One of the rhesus macaque alleles had identical sequences to one of the crab-eating macaque alleles, and the phylogenetic analysis demonstrated that the *ULBP4/RAET1E* alleles were widely diverged. None of the alleles identified in this study were identical to the previously reported sequence NC007861, which was derived from an individual of Indian rhesus macaque. Given that we analyzed rhesus macaques of Burmese origin in this study, and allele distribution of MHC-related polymorphic genes are well known to be largely dependent on the habitat regions, the extent of diversity and variation in *ULBP4/RAET1E* may be further expanded.

It was demonstrated that the diversity of *ULBP4/RAET1E* in the Old World monkeys was much higher than that of human *ULBP4/RAET1E*. It is possible that the genes in the *ULBP/RAET1* locus, in particular, *ULBP4/RAET1E* and *ULBP/RAET1*s, might be highly polymorphic in the

Old World monkeys. We therefore investigated ten unrelated rhesus macaque subjects, in which we had detected 16 *ULBP4/RAET1E* alleles for polymorphisms in the adjacent *ULBP/RAET1* genes. We found one *ULBP1/RAET1I* allele, seven *ULBP2/RAET1H* alleles, and one *ULBP3/RAET1N* allele in these subjects. The observation suggested that *ULBP4/RAET1E* was highly polymorphic as compared to the adjacent *ULBP/RAET1* genes.

We revealed a high degree of polymorphism in the *ULBP4/RAET1E* of the rhesus and crab-eating macaques, although about half of the polymorphisms were synonymous changes (Table 2). Albeit the expression of the ULBP4/RAET1E molecule is known to be involved in the recognition of tumor cells by the NKG2D receptor (Cao et al. 2008; Kong et al. 2009), the functional significance of the polymorphisms in the extracellular domain of the ULBP4/RAET1E molecules remained unknown. To investigate a possible role of the polymorphisms, we have created a 3-D structure model of rhesus ULBP4/RAET1E molecule by using the structure data of human ULBP3/RAET1N in complex with NKG2D (Radaev et al. 2001) as the reference. As shown in Fig. 3, only one polymorphic site at 173 was on the surface of the α helix pointing to the NKG2D receptor, five sites at 59, 136, 144, 161, and 165 were positioned outside the α helix, and only two sites at 32 and 91 were mapped on the β sheet in the groove. The other polymorphic sites were on the β sheet outside of the groove or were not on the surface of the α helix. In addition, expression of *ULBP4/RAET1E* is predominantly found in the skin and tumor tissues and not induced by viral infection in normal cells (Chalupny et al. 2003; Eagle et al. 2006). These observations suggest that the polymorphisms are unlikely to be involved in the differential presentation of characteristic small molecules bound by the ULBP4/RAET1E molecules, as found in the presentation of antigenic peptides by the MHC molecules. Nevertheless, highly prevalent polymorphisms leading to amino acid replacements suggest that a selection pressure had operated on the configuration of diversity in *ULBP4/RAET1E*.

Of particular interest in this study was the rhesus macaque allele *Mamu-ULBP4*8*, which was supposed to contain a stop codon in the exon 2 coding sequence that would truncate the most part of the molecule. This is the first report of a non-functional *ULBP/RAET1* allele in primates; however, a similar situation was reported for another NKG2D ligand gene, *MIC*. For example, a specific human *MIC* haplotype linked to HLA-B*048 consists of non-functional *MIC* genes, in which *MICA* was deleted and *MICB* contained a termination codon (Ota et al. 2000); the non-functional *MIC* haplotype is widely distributed in the East Asian populations (Komatsu-Wakui et al. 2001). It is interesting to note that there are two distinct and polymorphic genes for *MIC* in the rhesus macaque, *MICA* (previously designated as *MIC1* and *MIC3*) and *MICB* (previous *MIC2*); however, they are not considered to be orthologous to the human *MICA* and *MICB* genes, respectively (Seo et al. 1999, 2001; Doxiadis et al. 2007; Averdam et al. 2007). Because members of the MIC and ULBP/RAET1 molecules are structurally related (Li et al. 2002), there is a functional redundancy in the recognition by NKG2D, and thus, the presence of a null allele had been allowed during the evolution of primates.

In the present study, we demonstrated the *ULBP4/RAET1E* allelic polymorphisms not only in the rhesus macaque but also in the crab-eating macaque. Although the localization of *ULBP4/RAET1E* in the crab-eating macaque

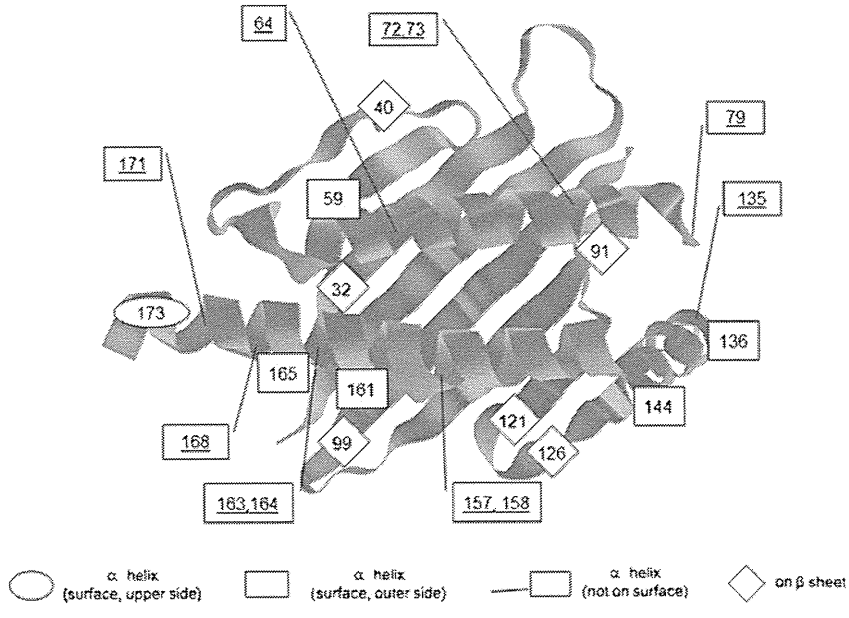

Fig. 3 Mapping of polymorphic sites on the structure model of the macaque ULBP4/RAET1E molecule. Polymorphic sites found in the Old World monkeys were mapped on the 3-D structure model of ULBP4/RAET1E. Residues on the upper and outer sides of the α helix structure were indicated by a *circle* and *squares*, respectively. Residues not found on the surface of the α helix were *underlined*, and those on the β sheet structure were represented by *rhombi*

genome is unknown, a homology search showed that a *Mafa-MICH3* gene (AY032639) was homologous to *Mafa-ULBP4/RAET1E* because the nucleotide sequences of *Mafa-ULBP4*1.1* showed a 96% homology to *Mafa-MICH3*. Similarly, nucleotide sequences of a chimpanzee gene, *Patr-MICH3* (AY032638), showed a 94% homology to the rhesus *ULBP4/RAET1E*. These findings strongly suggest that *MICH3* in the crab-eating macaque and chimpanzee is orthologous to *ULBP4/RAET1E* in the human and rhesus macaque.

In conclusion, we revealed a large diversity of *ULBP4/RAET1E* in two related species of the Old World monkey. Because there were extremely large polymorphisms in the extracellular domain of the ULBP4/RAET1E molecule in the Old World monkey, which was larger than that in the human, the functional impact of the polymorphisms and its significance in the evolution of primates should be investigated in future studies.

Acknowledgments We thank Ms. Yukiko Ueda for her technical assistance. This work was supported, in part, by research grants from the Ministry of Health, Labor and Welfare, Japan; the Japan Health Science Foundation; the program of Founding Research Centers for Emerging and Reemerging Infection Disease; the program of Research on Publicly Essential Drugs and Medical Devices; grants-in-aid for scientific research from the Ministry of Education, Culture, Sports, Science, and Technology (MEXT), Japan; a support for women researchers from the Tokyo Medical and Dental University; and a grant from the Life Science Institute Foundation.

References

Antoun A, Jobson S, Cook M, O'Callaghan CA, Moss P, Briggs DC (2010) Single nucleotide polymorphism analysis of the NKG2D ligand cluster on the long arm of chromosome 6: extensive polymorphisms and evidence of diversity between human populations. Hum Immunol 71:610–620

Averdam A, Seelke S, Grützner I, Ronser C, Roos C, Westphal N, Stahl-Hennig C, Muppala V, Schrod A, Sauermann U, Dressel R, Walter L (2007) Genotyping and segregation analyses indicate the presence of only two functional MIC genes in rhesus macaques. Immunogenetics 59:247–251

Bacon L, Eagle RA, Meyer M, Easom N, Young NT, Trowsdale J (2004) Two human ULBP/RAET1 molecules with transmembrane region are ligands for NKG2D. J Immunol 173:1078–1084

Bauer S, Groh V, Wu J, Steinle A, Phillips JH, Lanier LL, Spies T (1999) Activation of NK cells and T cells by NKG2D, a receptor for stress-inducible MICA. Science 285:727–729

Cao W, Xi X, Wang Z, Dong L, Hao Z, Cui L, Ma C, He W (2008) Four novel ULBP splice variants are ligands for human NKG2D. Int Immunol 20:981–991

Chalupny NJ, Sutherland CL, Lawrence WA, Rein-Weston A, Cosman D (2003) ULBP4 is a novel ligand for human NKG2D. Biochem Biophys Res Commun 305:129–135

Cosman D, Müllberg J, Sutherland CL, Chin W, Armitage R, Fanslow R, Kubin M, Chalupny NJ (2001) ULBPs, novel MHC class I–related molecules, bind to CMV glycoprotein UL16 and stimulate NK cytotoxicity through the NKG2D receptor. Immunity 14:123–133

Doxiadis GGM, Heijmans CM, Otting N, Bontrop RE (2007) MIC gene polymorphism and haplotype diversity in rhesus macaques. Tissue Antigens 69:212–219

Eagle RA, Traherne JA, Ashiru O, Wills MR, Trowsdale J (2006) Regulation of NKG2D ligand gene expression. Hum Immunol 67:1159–1169

Eagle RA, Flack G, Warford A, Martinez-Borra J, Jafferji I, Traherne JA, Ohashi M, Boyle LH, Barrow AD, Caillat-Zucman S, Young NT, Trowsdale J (2009a) Celllar expression, trafficking, and function of two isoforms of human ULBP5/RAET1G. Pros ONE 4:e4503

Eagle RA, Traherne JA, Hair JR, Jafferji I, Trowsdale J (2009b) ULBP6/RAET1L is an additional human NKG2D ligand. Eur J Immunol 39:3207–3216

Gibbs RA, Rogers J, Katze MG et al (2007) Evolutionary and biomedical insights from the rhesus macaque genome. Science 316:222–234

Huber I, Walter L, Wimmer R, Pasantes JJ, Günther E, Schempp W (2003) Cytogenetic mapping and orientation of the rhesus macaque MHC. Cytogenet Genome Res 103:144–1449

Komatsu-Wakui M, Tokunaga K, Ishikawa Y, Leelayuwat C, Kashiwase K, Tanaka H, Moriyama S, Nakajima F, Park MH, Jia GJ, Chimge NO, Sideltseva EW, Juji T (2001) Wide distribution of the MICA-MICB null haplotype in East Asians. Tissue Antigens 57:1–8

Kondo M, Maruoka T, Otsuka N, Kasamatsu J, Fugo K, Hanzawa N, Kasahara M (2010) Comparative genomic analysis of mammalian NKG2D ligand family genes provides insights into their origin and evolution. Immunogenetics 62:441–450

Kong Y, Cao W, Xi X, Ma C, Cui L, He W (2009) The NKG2D ligand ULBP4 binds to TCRgamma9/delta2 and induces cytotoxicity to tumor cells through both TCRgammadelta and NKG2D. Blood 114:310–317

Kulski JK, Anzai T, Shiina T, Inoko H (2004) Rhesus macaque class I duplicon structures, organization, and evolution within the alpha block of the major histocompatibility complex. Mol Biol Evol 21:2079–2091

Li P, McDermott G, Strong RK (2002) Crystal structures of RAE-1β and its complex with the activating immunoreceptor NKG2D. Immunity 16:77–86

Liu QY, Wang XX, Zhang JZ, Chen WH, He XW, Lin Y, Wang JF, Zhu Y, Hu SN, Wang XN (2007) Mapping cynomolgus monkey MHC class I district on chromosome 6p13 using pooled cDNAs. Biotech Histochem 82:267–272

Naruse KT, Chen Z, Yanagida R, Yamashita T, Saito Y, Mori K, Akari H, Yasutomi Y, Miyazawa M, Matano T, Kimura A (2010) Diversity of MHC class I genes in Burmese-origin rhesus macaque. Immunogenetics 62:601–611

Ota M, Bahram S, Katsuyama Y, Saito S, Nose Y, Sada M, Ando H, Inoko H (2000) On the MICA deleted-MICB null, HLA-B*4801 haplotype. Tissue Antigens 56:268–271

Otting N, Otting N, deVos-Rouweler AJM, Heijmans CMC, de Groot NG, Doxiadis GGM, Bontrop RE (2007) MHC class I A region diversity and polymorphism in macaque species. Immunogenetics 59:367–375

Pappworth IY, Wang EC, Rowe M (2007) The switch from latent to productive infection in Epstein-Barr virus-infected B cell is associated with sensitization to NK cell killing. J Virol 1:474–482

Pende D, Rivera P, Marcenaro S, Chang CC, Biassoni R, Conte R, Kubin M, Cosman D, Ferrone S, Moretta L, Moretta A (2002) Major histocompatibility complex class I-related chain A and UL16-binding protein expression on tumor cell lines of different histotypes: analysis of tumor susceptibility to NKG2D-dependent natural killer cell cytotoxicity. Cancer Res 62:6178–6186

Radaev S, Rostro B, Brooks AG, Colonna M, Sun PD (2001) Conformational plasticity revealed by the cocrystal structure of NKG2D and its class I MHC-like ligand ULBP3. Immunity 5:1039–1049

Radosavljevic M, Cuillerier B, Wilson MJ, Clement O, Wicker S, Gilfillan S, Beck S, Trowsdale J, Bahram S (2001) A cluster of ten novel MHC class I related genes on human chromosome 6q24.2-q25.3. Genomics 79:114–123

Raulet DH (2003) Roles of the NKG2D immunoreceptor and its ligands. Nat Rev Immunol 3:781–790

Romphruk AV, Romphruk A, Naruse TK, Raroengjai S, Puapairoj C, Inoko H, Leelayuwat C (2009) Polymorphisms of NKG2D ligands: diverse RAET1/ULBP genes in northeastern Thais. Immunogenetics 61:611–617

Seo JW, Bontrop R, Walter L, Günther E (1999) Major histocompatibility complex-linked MIC genes in rhesus macaques and other primates. Immunogenetics 50:358–362

Seo JW, Walter L, Günther E (2001) Genomic analysis of MIC genes in rhesus macaques. Tissue Antigens 58:159–165

Ward J, Bonaparte M, Sacks J, Guterman J, Fogli M, Mavilio D, Barker E (2007) HIV modulates the expression of ligands important in triggering natural killer cell cytotoxic responses on infected primary T-cell blasts. Blood 110:1207–1214

Wu J, Song Y, Bakker ABH, Bauer S, Spies T, Lanier LL, Phillips JH (1999) An activating immune receptor complex formed by NKG2D and DAP 10. Science 285:730–732

Journal of General Virology (2011), 92, 2272–2280 DOI 10.1099/vir.0.031229-0

Common marmoset (*Callithrix jacchus*) as a primate model of dengue virus infection: development of high levels of viraemia and demonstration of protective immunity

Tsutomu Omatsu,[1] Meng Ling Moi,[1] Takanori Hirayama,[1] Tomohiko Takasaki,[1] Shinichiro Nakamura,[2] Shigeru Tajima,[1] Mikako Ito,[1] Tomoyuki Yoshida,[3] Akatsuki Saito,[3] Yuko Katakai,[3,4] Hirofumi Akari[3]† and Ichiro Kurane[1]

Correspondence
Ichiro Kurane
kurane@nih.go.jp
Hirofumi Akari
akari@pri.kyoto-u.ac.jp

[1]Department of Virology I, National Institute of Infectious Diseases, 1-23-1 Toyama, Shinjuku-ku, Tokyo 162-8640, Japan

[2]Research Center for Animal Life Science, Shiga University of Medical Science, Seta Tsukinowa-cho, Otsu, Shiga 520-2192, Japan

[3]Laboratory of Disease Control, Tsukuba Primate Research Center, National Institute of Biomedical Innovation, 1 Hachimandai, Tsukuba, Ibaraki 305-0843, Japan

[4]Corporation for Production and Research of Laboratory Primate, National Institute of Biomedical Innovation, 1 Hachimandai, Tsukuba, Ibaraki 305-0843, Japan

Received 4 February 2011
Accepted 19 June 2011

Dengue virus (DENV) causes a wide range of illnesses in humans: dengue fever (DF), dengue hemorrhagic fever (DHF) and dengue shock syndrome (DSS). Animal models that constantly develop high levels of viraemia are required for the development of protective and preventive measures. Common marmosets (*Callithrix jacchus*) demonstrated high levels of viraemia after inoculation with clinical isolates of four serotypes of DENV; in particular, over 10^6 genome copies ml^{-1} after inoculation with DENV-2. Non-structural protein 1 and DENV-specific IgM and IgG antibodies were consistently detected. The DENV-2 genome was detected in lymphoid organs including the lymph nodes, spleen and thymus, and also in non-lymphoid organs. DENV antigen was detected by immunohistochemistry in the liver and spleen from inoculated marmosets. Four marmosets were reinoculated with DENV-2 at 33 weeks after primary inoculation with DENV-2. The DENV-2 genome was not detected in any of these marmosets, indicating protection from a secondary infection. The results indicate that common marmosets are highly sensitive to DENV infection, and suggest that marmosets could be a reliable primate model for the evaluation of candidate vaccines.

INTRODUCTION

Dengue virus (DENV) is an arthropod-borne flavivirus and is a serious cause of morbidity and mortality in the world. Approximately 2.5 billion people living in tropical and subtropical areas are at risk of DENV infection. Infection with any one of the four serotypes of DENV (DENV1–4) causes a range of symptoms: classical dengue fever (DF), and the sometimes fatal dengue hemorrhagic fever (DHF) and dengue shock syndrome (DSS). DF is an acute febrile illness, characterized by headache, rash, retro-orbital pain, arthralgia and myalgia. DHF is characterized by capillary leakage, thrombocytopenia, haemorrhagic manifestations, hypotension and liver parenchyma necrosis. When profound plasma leakage results in shock, the disease is called DSS (Halstead, 2007; WHO, 2002). No vaccines or specific antiviral drugs are currently available.

Animal models of DENV could facilitate the development of vaccines and anti-dengue viral agents (Bente & Rico-Hesse, 2006). Mouse models have proved to be useful in therapeutics and vaccine efficacy studies (Balsitis *et al.*, 2010; Shrestha *et al.*, 2010). However, limitations of these models include the usage of immunocompromised mice and the development of only limited levels of viraemia in immunocompetent mice, even when high titres of DENV

†Present address: Section of Comparative Immunology and Microbiology, Center for Human Evolution Modelling Research, Primate Research Institute, Kyoto University, Inuyama, Aichi 484-8506, Japan.

were inoculated. These aspects necessitate the development of immunocompetent animal models that are more relevant to DENV infection in humans, with the capability of supporting high levels of viral replication and antibody (Ab) response, and with additional advantages such as availability, ease of maintenance and handling. Non-human primates, rhesus monkeys, cynomolgus monkeys and owl monkeys, have been used in the evaluation of candidate vaccines (Koraka *et al.*, 2007); however, not all non-human primate models develop overt levels of viraemia (Ito *et al.*, 2010). It has been reported that disease severity is related to high levels of viraemia, and, reduction in viraemia is associated with reduced disease severity (Libraty *et al.*, 2002a). Neutralizing antibodies play a key role in protection and is an indicator of protective immunity as well as vaccine efficacy. A suitable animal model that consistently develops high levels of viraemia would provide a useful tool in addressing fundamental issues regarding vaccine development.

As viraemia is a critical parameter in assessing vaccine efficacy, establishment of models with close evolutionary proximity to humans would offer a valuable tool. In the present study, we attempt to establish a new animal model of DENV infection using common marmosets (*Callithrix jacchus*). Common marmosets are a small New World monkey that could be maintained with relative ease in captivity as compared with many other non-human primates. Subcutaneous inoculation of common marmosets with DENV consistently induces high levels of viraemia and Ab response. Marmosets that received a secondary inoculation with DENV-2 at 33 weeks after the primary inoculation did not develop detectable levels of viraemia. The results suggest that marmosets are a potentially reliable DENV infection model for the development of vaccine and anti-DENV therapeutics.

RESULTS

Infection of marmosets with four serotypes of DENV

Marmosets were subcutaneously inoculated with clinical isolates of DENV: 3.5×10^7 p.f.u. of DENV-1 (02-17/1 strain), 6.7×10^7 p.f.u. of DENV-2 (DHF0663 strain), 4.5×10^6 p.f.u. of DENV-3 (DSS1403 strain) and 1.5×10^6 p.f.u. of DENV-4 (05-40/1 strain). The strains DENV-1 02-17/1, DENV-2 DHF0663, DENV-3 DSS1403 and DENV-4 05-40/1 were clinical isolates that were propagated for less than four passages on C6/36 cells. Levels of dengue viral RNA (dengue vRNA) were assessed in plasma at various time points (Table 1, experiment 1). Dengue vRNA was detected in plasma samples from the marmosets on days 3 and 5 after inoculation. For each of the four animals (D1-1, D2-1, D3-1 and D4-1), the plasma levels of vRNA reached 5.0×10^5 copies ml^{-1} on day 5, 1.6×10^7 copies ml^{-1} on day 3, 5.5×10^4 copies ml^{-1} on day 5 and 2.5×10^4 copies ml^{-1} on day 3, respectively.

The level of non-structural protein 1 (NS1) in plasma samples was assessed by ELISA (Fig. 1a). NS1 was detected in plasma samples from D1-1, D2-1 and D3-1, and peaked on days 3–10 for D1-1, and on day 3 for D2-1 and D3-1. The results demonstrated that DENV-2 induced high levels of viraemia, and DENV-2 was, thus, used in the next series of experiments.

Infection of marmosets with four different doses of DENV-2

Four marmosets were inoculated with DENV-2 (DHF0663 strain) at two different doses; D2-2 and D2-3 with 4.4×10^7 p.f.u., and D2-4 and D2-5 with 1.8×10^5 p.f.u. Dengue vRNA was detected at levels of 10^6–10^7 copies ml^{-1} in plasma samples from all the marmosets on day 3 (Table 1, experiment 2). NS1 antigen was also detected in plasma samples from all the marmosets (Fig. 1d).

Four marmosets were then inoculated with lower doses of DENV-2 (DHF0663 strain); D2-6 and D2-7 with 1.8×10^4 p.f.u., and D2-8 and D2-9 with 1.8×10^3 p.f.u. Dengue vRNA was detected on days 2, 4 and 7 in all the four marmosets (Table 1, experiment 3). The plasma levels of vRNA reached the peak levels approximately 10^6 copies ml^{-1} in marmosets inoculated with 1.8×10^4 p.f.u. and approximately 5×10^5 copies ml^{-1} in those inoculated with 1.8×10^3 p.f.u. NS1 antigen was detected in plasma samples from all the marmosets (Fig. 1g). The results in experiments 2 and 3 indicate that marmosets inoculated with $\geqslant 1.8 \times 10^3$ p.f.u. developed viraemia at levels of more than 3.7×10^5 copies ml^{-1}.

Infection of marmosets with two other strains of DENV-2

Two other strains of DENV-2 were examined for the ability to induce viraemia. Marmosets D2-10 and D2-11 were inoculated with 1.2×10^5 p.f.u. of Jam/77/07 strain, and D2-12 and D2-13 with 1.9×10^5 p.f.u. of Mal/77/08 strain. The DENV-2 strains, Jam/77/07 and Mal/77/08, were clinical DENV strains that were propagated less than four passages on C6/36 cells. Dengue vRNA was detected in plasma samples from all four marmosets on days 2, 4 and 7, and the peak levels reached over 10^6 copies ml^{-1} on day 4 (Table 1, experiment 4). NS1 antigen was detected in plasma samples from all marmosets (Fig. 1j). The results in experiments 2, 3 and 4 indicate that marmosets developed similarly high levels of viraemia after inoculation with three different strains of DENV-2.

Antibody responses in marmosets after inoculation with DENV

DENV-specific IgM and IgG Ab responses were examined by ELISA after inoculation with DENV. In experiment 1, specific IgM Ab was first detected on day 5 for D1-1, D2-1

Table 1. Levels of dengue vRNA in plasma from marmosets inoculated with DENV

–, vRNA below the limit of detection using RT-PCR; NT, not tested.

Animal ID	Virus strain	Inoculated dose		Dengue vRNA copy numbers (copies ml^{-1})									
		p.f.u. per dose	copies per dose	Days after inoculation									
				0	2	3	4	5	7	8	10	14	21
Primary inoculation													
Experiment 1													
D1-1	02-17/1	3.5×10^7	4.6×10^8	–	NT	3.8×10^5	NT	5.0×10^5	–	NT	–	–	*
D2-1	DHF0663	6.7×10^7	8.2×10^8	–	NT	1.6×10^7	NT	1.0×10^5	–	NT	–	–	*
D3-1	DSS1403	4.5×10^6	2.5×10^8	–	NT	–	NT	5.5×10^4	–	NT	–	–	*
D4-1	05-40/1	1.5×10^6	1.1×10^9	–	NT	2.5×10^4	NT	–	–	NT	–	–	*
Experiment 2													
D2-2	DHF0663	4.4×10^7	5.4×10^8	–	NT	1.2×10^7	NT	NT	–	NT	NT	–	–
D2-3				–	NT	8.6×10^6	NT	NT	–	NT	NT	–	–
D2-4		1.8×10^5	2.2×10^6	–	NT	6.1×10^6	NT	NT	–	NT	NT	–	–
D2-5				–	NT	9.5×10^6	NT	NT	3.5×10^5	NT	NT	–	–
Experiment 3													
D2-6	DHF0663	1.8×10^4	2.2×10^5	–	3.4×10^5	NT	2.0×10^6	NT	5.1×10^4	NT	NT	–	*
D2-7				–	3.8×10^5	NT	9.4×10^5	NT	2.8×10^4	NT	NT	–	*
D2-8		1.8×10^3	2.2×10^4	–	2.2×10^4	NT	3.7×10^5	NT	1.4×10^4	NT	NT	–	*
D2-9				–	6.2×10^4	NT	6.9×10^5	NT	2.2×10^5	NT	NT	–	*
Experiment 4													
D2-10	Jam/77/07	1.2×10^5	1.4×10^7	–	1.0×10^6	NT	2.8×10^6	NT	4.6×10^4	NT	NT	–	–
D2-11				–	8.7×10^5	NT	2.0×10^6	NT	4.9×10^4	NT	NT	–	–
D2-12	Mal/77/08	1.9×10^5	7.1×10^6	–	4.8×10^6	NT	9.6×10^6	NT	5.8×10^3	NT	NT	–	–
D2-13				–	2.0×10^6	NT	7.0×10^6	NT	4.7×10^3	NT	NT	–	–
Experiment 5													
D2-14	DHF0663	6.7×10^7	8.2×10^8	–	8.3×10^6	5.9×10^6	*	*	*	*	*	*	*
D2-15				–	7.8×10^6	NT	3.7×10^6	3.5×10^5	*	*	*	*	*
D2-16				–	2.3×10^7	NT	6.5×10^6	NT	2.8×10^5	-	*	*	*
D2-17				–	3.1×10^7	NT	3.6×10^6	NT	6.0×10^4	NT	NT	–	–
Secondary inoculation													
Experiment 6													
D2-2	DHF0663	1.8×10^5	2.2×10^6	–	–	NT	–	NT	–	NT	NT	–†	–
D2-3				–	–	NT	–	NT	–	NT	NT	–†	–
D2-4				–	–	NT	–	NT	–	NT	NT	–†	–
D2-5				–	–	NT	–	NT	–	NT	NT	–†	–

*The marmosets were sacrificed and no samples were collected.
†Indicates day 15.

and D3-1, and, on day 7 for D4-1 (Fig. 1b). IgM Ab reached peak levels on day 10 for D1-1, D2-1 and D3-1. IgG Ab was first detected on day 10 for all four animals, and IgG Ab levels increased thereafter (Fig. 1c). Although DENV-4 inoculation induced only low levels of viraemia, both DENV-specific IgM and IgG Abs were induced. DENV-specific IgM and IgG were similarly detected in all the marmosets inoculated with DENV-2 in experiments 2, 3 and 4 (Fig. 1e, h, k for IgM, and Fig. 1f, i, l for IgG). These results, along with those shown in Table 1 and Fig. 1(b, c), indicate that DENV propagated and induced specific IgM and IgG antibodies in marmosets.

Detection of DENV in organs

The distribution of DENV in organs was examined. Four marmosets were inoculated with 6.7×10^7 p.f.u. of DENV-2 (DHF0663 strain). One animal each was euthanized and the organs collected on days 3, 5, 8 and 14. All marmosets demonstrated viraemia (Table 1, experiment 5). NS1 antigen was also detected in all four marmosets (Fig. 1m). IgM and IgG were first detected on day 5 and day 8, respectively (Fig. 1n, o). The results indicate that DENV-2 infection was established in these four marmosets.

Levels of DENV-2 vRNA were assessed in thymus, lung, liver, kidneys, pancreas, spleen, lymph nodes, urinary

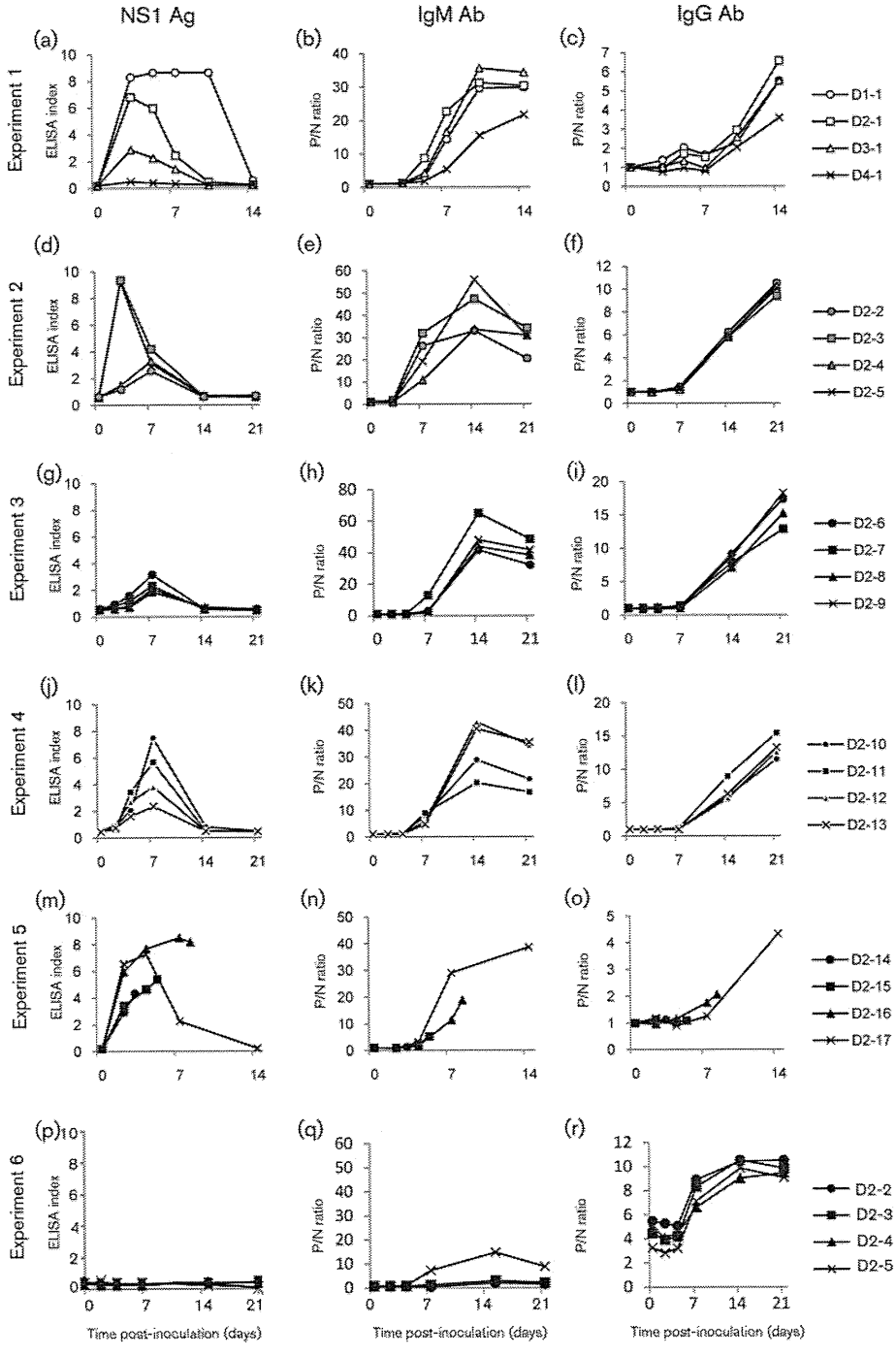

Fig. 1. Levels of DENV NS1 and DENV-specific IgM and IgG Abs in plasma samples from marmosets inoculated with DENV. ELISA index of NS1 antigen (a, d, g, j, m and p), P/N ratio of DENV-specific IgM Ab (b, e, h, k, n and q) and P/N ratio of DENV-specific IgG Ab (c, h, i, l, o and r) in plasma samples from marmosets inoculated with DENV in experiment 1 (a–c), experiment 2 (d–f), experiment 3 (g–i), experiment 4 (j–l), experiment 5 (m–o) and experiment 6 (p–r). Day 0 was defined as the day of virus inoculation.

bladder and bone marrow on days 3, 5, 8 and 14 after inoculation (Table 2). DENV-2 vRNA was detected in mandibular, axillary, mesenteric and inguinal lymph nodes from all animals. DENV-2 vRNA was detected in thymus on days 3, 5 and 8, and in spleen on days 5, 8 and 14. DENV-2 vRNA was also detected in the non-lymphoid

Table 2. Levels of dengue vRNA in organs from marmosets inoculated with DENV-2 DHF0663 strain

–, vRNA below the limit of detection using RT-PCR.

Organs	Dengue vRNA copy numbers in organs (copies μg^{-1} of total RNA)			
	Days after inoculation with DENV-2			
	3	5	8	14
Viraemia titres* (copies ml^{-1})	5.9×10^6	3.5×10^5	–	–
Lymph node				
Mandibular	–	1.4×10^4	9.2×10^4	–
Axillary	4.3×10^4	6.4×10^3	5.1×10^4	2.3×10^3
Mesenteric	–	2.9×10^4	4.2×10^4	8.8×10^3
Inguinal	8.8×10^3	3.0×10^4	4.9×10^4	2.9×10^3
Thymus	5.7×10^3	1.5×10^4	9.5×10^4	–
Spleen	–	2.8×10^4	1.4×10^5	3.0×10^4
Bone marrow	3.3×10^3	–	–	–
Lung	2.2×10^3	1.9×10^4	–	1.5×10^4
Liver	8.0×10^1	–	8.2×10^3	–
Kidney (right)	–	–	–	9.8×10^4
Kidney (left)	2.3×10^3	1.6×10^2	1.9×10^2	2.6×10^5
Pancreas	3.6×10^4	4.4×10^2	6.6×10^3	–
Urinary bladder	–	1.0×10^4	–	6.6×10^3

*Viraemia titres in serum samples at the day of sacrifice (copies ml^{-1}).

organs: lungs, liver, kidneys, pancreas and urinary bladder. The results suggest that DENV-2 propagated in the lymphoid organs and non-lymphoid organs.

The presence of DENV-infected cells was examined in the liver and spleen by immunohistochemistry. DENV antigen-positive cells were detected in Kupffer cells in the liver (Fig. 2a) and in lymphocytes and macrophages in the spleen (Fig. 2b). The results confirm that DENV infection was established in marmosets after inoculation with DENV.

Absence of dengue vRNA after a secondary inoculation with DENV-2

Four marmosets (D2-2, D2-3, D2-4 and D2-5) were reinoculated with 1.8×10^5 p.f.u. of DENV-2 at 33 weeks after primary inoculation with DENV-2. The levels of dengue vRNA were assessed on days 0, 2, 4, 7, 15 and 21 after the secondary inoculation (Table 1, experiment 6). Dengue vRNA was not detected in any of the marmosets on 2–21 days after inoculation. NS1 antigen was not detected in any of the four marmosets after secondary inoculation with DENV-2 (Fig. 1p).

Robust IgG responses were detected by ELISA in all the four marmosets (Fig. 1r). Neutralizing Ab was examined in the four marmosets (D2-2–D2-5) after the primary and secondary inoculations (Table 3, experiment 2). Neutralizing Ab was first detected on day 14 after the primary inoculation. Neutralizing Ab titres were at levels of 1:20–1:80 before the secondary inoculation. The titres increased from 1:160 to 1:640 on day 7 after the secondary inoculation (Table 3, experiment 6). The results indicate that primary inoculation with DENV-2 induced protective immunity to DENV-2.

DISCUSSION

Non-human primates and rodents have been used as animal models for the evaluation of candidate dengue vaccines. Although Ab responses and kinetics of viraemia in these models, in particular in macaques, were similar to those in human DENV infection, viraemia levels were modest and apparent clinical signs were absent (Ito *et al.*, 2010; Marchette *et al.*, 1973). There remains a need for the development of a reliable animal model that better recapitulates DENV infection in humans. Several aspects, including incubation period, duration of viraemia and Ab responses in experimentally infected marmosets in the present studies appear to recapitulate DENV infection in humans (Vaughn *et al.*, 1997).

DENV infection induces the NS1 antigen in blood (Alcon *et al.*, 2002; Flamand *et al.*, 1999; Libraty *et al.*, 2002b). As reported in human studies (Mackenzie *et al.*, 1996), the NS1 antigen was detected in DENV-infected marmosets, indicating DENV replication. Plasma viraemia levels reached a peak of approximately 10^6 copies ml^{-1} on day 4 followed by gradual decline, with inoculation as low as 10^3 p.f.u. of DENV. In addition, using a subset of samples,

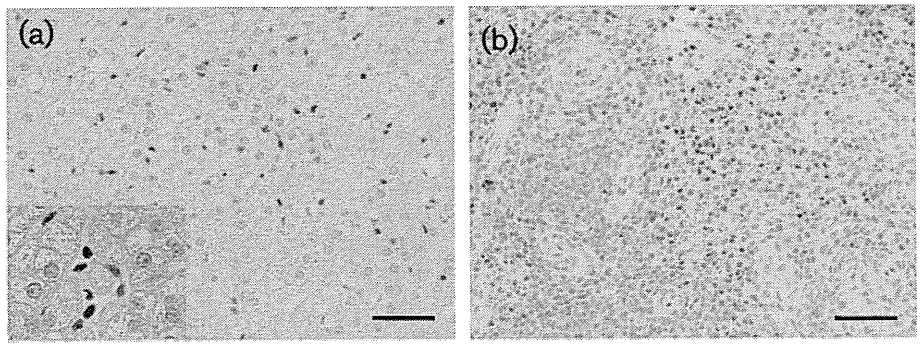

Fig. 2. Presence of DENV antigen in the liver and spleen of a marmoset inoculated with DENV. DENV antigen-positive cells were in the liver (a) and spleen (b) from marmoset D2-17. The inset (a) shows antigen-positive cells that correspond morphologically to the Kupffer cells. Kupffer cells were identified based on the morphological and localization characteristics of the cells; the cells were polygonal or spindal shaped, and were located in liver sinusoids. Bars, 50 μm.

peak viraemia titres were examined in three marmosets using the plaque titration method. Peak viraemia titres were constantly detected on days 3 and 4 after infection. Viraemia titres were 1.0×10^4 p.f.u. ml^{-1} (D2-6) and 1.0×10^3 p.f.u. ml^{-1} (D2-12) at 4 days post-inoculation, and 8.3×10^3 p.f.u. ml^{-1} (D2-14) at 3 days post-inoculation. Quantitative RT-PCR has proved to be useful in studies determining viraemia levels in other DENV animal models using rhesus macaque and mice (Bente *et al.*, 2005; Onlamoon *et al.*, 2010). Viraemia levels in marmosets determined by using quantitative real-time PCR (RT-PCR) and plaque assays were higher or at similar levels to those reported in other non-human primates (Bernardo *et al.*, 2008; Blair *et al.*, 2006; Goncalvez *et al.*, 2007; Guirakhoo *et al.*, 2004; Raviprakash *et al.*, 2008; Schiavetta *et al.*, 2003; Whitehead *et al.*, 2003). In the present study, all marmosets developed viraemia using inoculation doses from 10^7 to 10^3 p.f.u. per dose.

Although there was a tendency toward the development of differential viraemia patterns between the marmosets inoculated with 10^7–10^5 p.f.u. per dose and 10^4–10^3 p.f.u. per dose, further evaluations are needed to define the viraemia patterns between the two groups. The results indicate that a higher dose of viral inoculum does not necessarily lead to higher viraemia titres or longer viraemia durations. Overall, the results indicate that DENV infection was established after primary inoculation in marmosets. DENV viraemia was consistently detected in all of the experimentally infected marmosets using various DENV

Table 3. Neutralizing Ab titres to DENV-2 in marmosets after inoculation with DENV-2

NT, Indicates not tested.

Animal ID	Virus strain	Dose (p.f.u. per dose)	Neutralizing Ab titre							
			Days after inoculation with DENV-2							
			0	2	3	4	7	14	15	21
Primary inoculation										
Experiment 2										
D2-2	DHF0663	4.4×10^7	<20	NT	<20	NT	<20	80	NT	160
D2-3			<20	NT	<20	NT	<20	80	NT	80
D2-4		1.8×10^5	<20	NT	<20	NT	<20	160	NT	160
D2-5			<20	NT	<20	NT	<20	40	NT	80
Secondary inoculation										
Experiment 6										
D2-2	DHF0663	1.8×10^5	80	80	NT	40	640	NT	640	>1280
D2-3			40	80	NT	20	320	NT	640	640
D2-4			40	40	NT	80	160	NT	320	640
D2-5			20	20	NT	40	160	NT	320	320

strains isolated from human clinical samples at several of the inoculation doses. The results indicate that marmosets possess high sensitivity to DENV and could be a viable animal model for the evaluation of vaccine candidates and anti-DENV drugs.

In common marmosets, dengue vRNA was detected in lymphoid organs, lymph nodes, spleen, thymus and bone marrow, and also in non-lymphoid organs. DENV antigen-positive cells were detected in the spleen and liver of infected marmosets as in human patients (Bhamarapravati *et al.*, 1967; de Araújo *et al.*, 2009; Jessie *et al.*, 2004; Rosen *et al.*, 1999). Dengue vRNA was also detected in urine samples from DENV-infected marmosets (data not presented), as reported in human infection (Mizuno *et al.*, 2007; Poloni *et al.*, 2010). Of note, vRNA was detected in organs on day 14 when viraemia was no longer detected, as reported by other investigators (Marchette *et al.*, 1973). The results confirm propagation of DENV in inoculated marmosets.

Infection with one serotype of DENV induces life-long protective immunity to the same serotype in humans. Dengue vRNA and NS1 were not detected in plasma samples from marmosets that were reinoculated with DENV-2 at 33 weeks after primary inoculation (Table 1). The results indicate that protective immunity to the same serotype of DENV was induced by the primary infection as demonstrated in humans, and suggest that the marmoset model is potentially useful for evaluation of immunogenecity of candidate dengue vaccines. In contrast, using RT-PCR, viraemia was detected in all marmosets (D2-6, D2-7, D2-8 and D2-9) that were reinoculated with heterologous DENV serotypes (DENV-1 and DENV-3). Viraemia titres for D2-6 and D2-7 as assessed by RT-PCR were 5.1×10^4 copies ml^{-1} and 1.3×10^5 copies ml^{-1}, respectively, at day 7 post-inoculation with DENV-1, and viraemia titres for D2-8 and D2-9 were 3.8×10^5 copies ml^{-1} and 3.2×10^5 copies ml^{-1}, respectively, at day 7 post-inoculation with DENV-3 (M. L. Moi and others, unpublished data). Viraemia was not detected at day 7 after primary infection with DENV-1 and DENV-3 (Table 1). Although the results suggest that higher viraemia titres may have been induced in marmosets after secondary infection with heterologous DENV serotypes as compared with primary DENV infection, further studies using a greater number of marmosets are needed to address the clinical and pathophysiological aspects of heterologous secondary infection in marmosets. While other non-human primate models developed similar viraemia levels as marmosets shown in the present study (Guirakhoo *et al.*, 2004), the common marmoset model offers several advantages over other models for their use in research. These include small size (250–450 g), ease and lower cost of maintenance, availability and ease of handling which allows the introduction of flexibility into experimental procedures. Thus, common marmosets, in which high levels of viraemia were consistently detected upon DENV infection, could potentially provide a reliable and valuable model for evaluation of antiviral therapeutics and candidate vaccines against DENV.

METHODS

Cells. Vero cells were cultured in minimum essential medium (MEM; Sigma) with 10 % heat-inactivated FBS (Gibco) at 37 °C in 5 % CO_2. C6/36 cells were cultured in MEM with 10 % FBS and 1 % non-essential amino acids at 28 °C in 5 % CO_2.

Virus. DENV type 1 (DENV-1), 02-17/1 strain, DENV type 2 (DENV-2), DHF0663 strain (GenBank accession no. AB189122), D2/Hu/Jamaica/77/2007NIID (Jam/77/07) strain and D2/Hu/Maldives/77/2008NIID (Mal/77/08) strain, DENV type 3 (DENV-3), DSS1403 strain (GenBank accession no. AB189125) and DENV type 4 (DENV-4), 05-40/1 strain, were used for inoculation studies. The DENV-1 02-17/1 strain was isolated from an imported DF case from Indonesia. The DENV-2 DHF0663 strain was isolated from a DHF case in Indonesia. The DENV-2 Jam/77/07 and Mal/77/08 strains were isolated from imported DF cases from Jamaica and Maldives, respectively. The DENV-3 DSS1403 strain was isolated from a DSS case in Indonesia. The DENV-4 05-40/1 strain was isolated from an imported DF case from the Philippines. All DENV strains isolated from clinical samples were propagated with C6/36 cells and were used within four passages. Culture supernatant from infected C6/36 cells was centrifuged at 800 *g* for 5 min to remove cell debris, and then stored at −80 °C until use.

Infection of marmosets with DENV. A total of 20 male marmosets, weighing 258–512 g, were used. Marmosets were purchased from Clea Japan Inc. and caged singly at 27 ± 2 °C in 50 ± 10 % humidity with a 12 h light–dark cycle (lighting from 7:00 to 19:00) at Tsukuba Primate Research Center, National Institute of Biomedical Innovation, Tsukuba, Japan. Animals were fed twice a day with a standard marmoset diet (CMS-1M; CLEA Japan) supplemented with fruit, eggs and milk. Water was given *ad libitum*. The animals were in a healthy condition and confirmed to be negative for anti-DENV antibodies prior to primary DENV inoculation.

In experiment 1, the sensitivity of marmosets to each of the four serotypes of DENV was examined. Four marmosets were inoculated subcutaneously on the back with 3.5×10^7 p.f.u. of DENV-1 (02-17/1 strain), 6.7×10^7 p.f.u. of DENV-2 (DHF0663 strain), 4.5×10^6 p.f.u. of DENV-3 (DSS1403 strain) or 1.5×10^6 p.f.u. of DENV-4 (05-40/1 strain). Blood samples were collected before inoculation (day 0) and on days 3, 7, 10 and 14 after inoculation. Blood samples were used for the assessment of viraemia levels, IgG and IgM Abs, and the NS1 antigen level. All marmosets were euthanized on day 14 and organs were subjected to pathological examination.

In experiment 2, four marmosets were inoculated with DENV-2; two (D2-2 and D2-3) with 4.4×10^7 p.f.u. of DENV-2, DHF0663 strain, and two (D2-4 and D2-5) with 1.8×10^5 p.f.u. of DENV-2, DHF0663 strain. Blood samples were collected before inoculation (day 0) and on days 3, 7, 14 and 21 for the assessment of viraemia levels, IgG, IgM and the NS1 levels, and neutralizing Ab titres.

In experiment 3, four marmosets were used for the evaluation of their sensitivity to lower doses of DENV-2, DHF0663 strain; two (D2-6 and D2-7) with 1.8×10^4 p.f.u., and two (D2-8 and D2-9) with 1.8×10^3 p.f.u.

In experiment 4, four marmosets were inoculated with two other strains of DENV-2; two (D2-10 and D2-11) with 1.2×10^5 p.f.u. of Jam/77/07 strain, and two (D2-12 and D2-13) with 1.9×10^5 p.f.u. of Mal/77/08 strain. In these two experiments, blood samples were collected before inoculation (day 0) and on days 2, 4, 7, 14 and 21 for the assessment of viraemia levels, IgG, IgM and the NS1 levels.

In experiment 5, the distribution of DENV in various organs was examined. Four marmosets were inoculated with 6.7×10^7 p.f.u. of DENV-2, DHF0663 strain. One each was euthanized on days 3, 5, 8 or 14 after inoculation, and the organs collected for detection of dengue vRNA and histopathological analysis. Blood samples were collected from the animals before inoculation (day 0) and on days 2, 4, 7 and 13 for virus titration, IgG, IgM and the NS1 antigen detection.

In experiment 6, four marmosets used in experiment 2 were reinoculated with 1.8×10^5 p.f.u. of DENV-2, DHF0663 strain. Blood samples were collected on the day before inoculation (day 0) and on days 2, 4, 7, 15 and 21 for the assessment of viraemia levels and neutralizing Ab titres. Inoculation with DENV and blood drawing were performed under anaesthesia with 5 mg kg^{-1} of ketamine hydrochloride. Day 0 was defined as the day of virus inoculation.

All animal studies were conducted in accordance with 'Guides for animal experiments performed at National Institute of Infectious Diseases' approved by the Animal Welfare and Animal Care Committee of the National Institute of Infectious Diseases, Japan (approval nos 608011 and 609014), and 'National Institute of Biomedical Innovation rules and guidelines for experimental animal welfare' approved by the National Institute of Biomedical Innovation, Japan (approval nos 20-003 and 21-013).

Titration of vRNA in plasma and organs. Plasma samples were stored at −80 °C until use. Collected organs were homogenized by BioMasher (Nippi). Homogenized samples were suspended with 0.5 ml PBS(−) and centrifuged at 800 *g* for 5 min. After centrifugation, supernatants were collected and stored at −80 °C until use. vRNA was isolated from plasma and organ samples, using the High Pure Viral RNA kit (Roche Diagnostics). As housekeeping genes vary among tissues, experimental treatment and infection, total RNA was used to avoid specific expression profiles among housekeeping genes. Levels of dengue vRNA were determined by quantitative real-time RT-PCR as previously reported (Ito *et al.*, 2004). All RT-PCR assays were performed in duplicate.

Detection of DENV NS1, anti-DENV IgM and IgG Abs in plasma. Levels of NS1 in plasma samples were assessed by Platelia Dengue NS1 Ag assay (Bio-Rad). The assay was performed according to the manufacturer's instructions with modification to the applied volume of plasma. ELISA index was calculated by the formula: optical density (OD) of the test sample divided by the mean OD of the cut-off control (tested in duplicate). ELISA indexes of <1 and $\geqslant 1$ were considered to be negative and positive, respectively.

DENV-specific IgM Ab was detected by Dengue Fever IgM Capture ELISA (Focus) and DENV-specific IgG Ab was examined by Dengue IgG Indirect ELISA (PanBio) according to the manufacturer's instructions. The positive/negative (P/N) ratio was calculated by the formula: OD of the test sample divided by the OD of a negative sample. Plasma samples collected on the day of inoculation were used as the negative samples. P/N ratios of <2 and $\geqslant 2$ were considered to be negative and positive, respectively. All ELISAs were conducted in duplicates (Moi *et al.*, 2010a).

Titration of neutralizing Abs to DENV-2. Neutralizing Ab titres were determined by using plaque reduction neutralization tests with DENV-2, DHF0663 strain. Heat-inactivated serum samples were serially diluted twofold from 1:20 to 1:1250 with MEM supplemented with 2% FCS. Virus–Ab mixture was prepared by mixing 50 µl DENV-2 at titres of 1000 p.f.u. ml^{-1} with 50 µl of serially diluted serum samples. Control virus samples were prepared by mixing 50 µl DENV-2 at titres of 1000 p.f.u. ml^{-1} with 50 µl MEM supplemented with 2% FCS. Virus–Ab mixture was incubated at 37 °C for 1 h. One hundred microlitres of virus–Ab mixture was inoculated onto Vero monolayers into six-well plates. After 5 days of inoculation, cells were fixed and stained, and plaques were counted. Neutralization titre is expressed as the maximum dilution of plasma sample that yielded a >50% plaque reduction in the virus inoculum as compared with control virus sample (Moi *et al.*, 2010b).

Immunohistochemical analysis. The livers and spleens from marmosets were fixed in 10% neutral buffered formalin and embedded in paraffin. Paraffin-embedded tissues were cut into 4 µm sections. For immunohistochemical analysis, a series of sections was stained for DENV antigen using a marmoset polyclonal anti-DENV Ab conjugated with horseradish peroxidase. Sections were counterstained with haematoxylin.

ACKNOWLEDGEMENTS

This work was supported by grants from Research on Biological Resources and Animal Models for Drug Development (H19-Seibutsushigen-ippan-003), Research on Emerging and Re-emerging Infectious Diseases (H18-shinkou-ippan-009, H20-shinkou-ippan-015 and H23-shinkou-ippan-010) from the Ministry of Health, Labour and Welfare, Japan, and Grant-in-Aid for Scientific Research (B) no. 22390093 from the Ministry of Education, Culture, Sports, Science and Technology of Japan.

REFERENCES

Alcon, S., Talarmin, A., Debruyne, M., Falconar, A., Deubel, V. & Flamand, M. (2002). Enzyme-linked immunosorbent assay specific to Dengue virus type 1 nonstructural protein NS1 reveals circulation of the antigen in the blood during the acute phase of disease in patients experiencing primary or secondary infections. *J Clin Microbiol* **40**, 376–381.

Balsitis, S. J., Williams, K. L., Lachica, R., Flores, D., Kyle, J. L., Mehlhop, E., Johnson, S., Diamond, M. S., Beatty, P. R. & Harris, E. (2010). Lethal antibody enhancement of dengue disease in mice is prevented by Fc modification. *PLoS Pathog* **6**, e1000790.

Bente, D. A. & Rico-Hesse, R. (2006). Models of dengue virus infection. *Drug Discov Today Dis Models* **3**, 97–103.

Bente, D. A., Melkus, M. W., Garcia, J. V. & Rico-Hesse, R. (2005). Dengue fever in humanized NOD/SCID mice. *J Virol* **79**, 13797–13799.

Bernardo, L., Izquierdo, A., Prado, I., Rosario, D., Alvarez, M., Santana, E., Castro, J., Martínez, R., Rodríguez, R. & other authors (2008). Primary and secondary infections of *Macaca fascicularis* monkeys with Asian and American genotypes of dengue virus 2. *Clin Vaccine Immunol* **15**, 439–446.

Bhamarapravati, N., Tuchinda, P. & Boonyapaknavik, V. (1967). Pathology of Thailand haemorrhagic fever: a study of 100 autopsy cases. *Ann Trop Med Parasitol* **61**, 500–510.

Blair, P. J., Kochel, T. J., Raviprakash, K., Guevara, C., Salazar, M., Wu, S. J., Olson, J. G. & Porter, K. R. (2006). Evaluation of immunity and protective efficacy of a dengue-3 pre-membrane and envelope DNA vaccine in *Aotus nancymae* monkeys. *Vaccine* **24**, 1427–1432.

de Araújo, J. M., Schatzmayr, H. G., de Filippis, A. M., Dos Santos, F. B., Cardoso, M. A., Britto, C., Coelho, J. M. & Nogueira, R. M. (2009). A retrospective survey of dengue virus infection in fatal cases from an epidemic in Brazil. *J Virol Methods* **155**, 34–38.

Flamand, M., Megret, F., Mathieu, M., Lepault, J., Rey, F. A. & Deubel, V. (1999). Dengue virus type 1 nonstructural glycoprotein NS1 is secreted from mammalian cells as a soluble hexamer in a glycosylation-dependent fashion. *J Virol* **73**, 6104–6110.

Goncalvez, A. P., Engle, R. E., St Claire, M., Purcell, R. H. & Lai, C.-J. (2007). Monoclonal antibody-mediated enhancement of dengue virus infection *in vitro* and *in vivo* and strategies for prevention. *Proc Natl Acad Sci U S A* **104**, 9422–9427.

Guirakhoo, F., Pugachev, K., Zhang, Z., Myers, G., Levenbook, I., Draper, K., Lang, J., Ocran, S., Mitchell, F. & other authors (2004). Safety and efficacy of chimeric Yellow fever-dengue virus tetravalent vaccine formulations in nonhuman primates. *J Virol* **78**, 4761–4775.

Halstead, S. B. (2007). Dengue. *Lancet* **370**, 1644–1652.

Ito, M., Takasaki, T., Yamada, K., Nerome, R., Tajima, S. & Kurane, I. (2004). Development and evaluation of fluorogenic TaqMan reverse transcriptase PCR assays for detection of dengue virus types 1 to 4. *J Clin Microbiol* **42**, 5935–5937.

Ito, M., Mukai, R. Z., Takasaki, T., Kotaki, A. & Kurane, I. (2010). Antibody-dependent enhancement of dengue virus infection *in vitro* by undiluted sera from monkeys infected with heterotypic dengue virus. *Arch Virol* **155**, 1617–1624.

Jessie, K., Fong, M. Y., Devi, S., Lam, S. K. & Wong, K. T. (2004). Localization of dengue virus in naturally infected human tissues, by immunohistochemistry and in situ hybridization. *J Infect Dis* **189**, 1411–1418.

Koraka, P., Benton, S., van Amerongen, G., Stittelaar, K. J. & Osterhaus, A. D. (2007). Efficacy of a live attenuated tetravalent candidate dengue vaccine in naïve and previously infected cynomolgus macaques. *Vaccine* **25**, 5409–5416.

Libraty, D. H., Endy, T. P., Houng, H. S., Green, S., Kalayanarooj, S., Suntayakorn, S., Chansiriwongs, W., Vaughn, D. W., Nisalak, A. & other authors (2002a). Differing influences of virus burden and immune activation on disease severity in secondary dengue-3 virus infections. *J Infect Dis* **185**, 1213–1221.

Libraty, D. H., Young, P. R., Pickering, D., Endy, T. P., Kalayanarooj, S., Green, S., Vaughn, D. W., Nisalak, A., Ennis, F. A. & Rothman, A. L. (2002b). High circulating levels of the dengue virus nonstructural protein NS1 early in dengue illness correlate with the development of dengue hemorrhagic fever. *J Infect Dis* **186**, 1165–1168.

Mackenzie, J. M., Jones, M. K. & Young, P. R. (1996). Immunolocalization of the dengue virus nonstructural glycoprotein NS1 suggests a role in viral RNA replication. *Virology* **220**, 232–240.

Marchette, N. J., Halstead, S. B., Jr, Falkler, W. A., Jr, Stenhouse, A. & Nash, D. (1973). Studies on the pathogenesis of dengue infection in monkeys. 3. Sequential distribution of virus in primary and heterologous infections. *J Infect Dis* **128**, 23–30.

Mizuno, Y., Kotaki, A., Harada, F., Tajima, S., Kurane, I. & Takasaki, T. (2007). Confirmation of dengue virus infection by detection of dengue virus type 1 genome in urine and saliva but not in plasma. *Trans R Soc Trop Med Hyg* **101**, 738–739.

Moi, M. L., Takasaki, T., Kotaki, A., Tajima, S., Lim, C. K., Sakamoto, M., Iwagoe, H., Kobayashi, K. & Kurane, I. (2010a). Importation of dengue virus type 3 to Japan from Tanzania and Cote d'Ivoire. *Emerg Infect Dis* **16**, 1770–1772.

Moi, M. L., Lim, C. K., Kotaki, A., Takasaki, T. & Kurane, I. (2010b). Discrepancy in dengue virus neutralizing antibody titers between plaque reduction neutralizing tests with Fcγ receptor (FcγR)-negative and FcγR-expressing BHK-21 cells. *Clin Vaccine Immunol* **17**, 402–407.

Onlamoon, N., Noisakran, S., Hsiao, H. M., Duncan, A., Villinger, F., Ansari, A. A. & Perng, G. C. (2010). Dengue virus-induced hemorrhage in a nonhuman primate model. *Blood* **115**, 1823–1834.

Poloni, T. R., Oliveira, A. S., Alfonso, H. L., Galvão, L. R., Amarilla, A. A., Poloni, D. F., Figueiredo, L. T. & Aquino, V. H. (2010). Detection of dengue virus in saliva and urine by real time RT-PCR. *Virol J* **7**, 22.

Raviprakash, K., Wang, D., Ewing, D., Holman, D. H., Block, K., Woraratanadharm, J., Chen, L., Hayes, C., Dong, J. Y. & Porter, K. (2008). A tetravalent dengue vaccine based on a complex adenovirus vector provides significant protection in rhesus monkeys against all four serotypes of dengue virus. *J Virol* **82**, 6927–6934.

Rosen, L., Drouet, M. T. & Deubel, V. (1999). Detection of dengue virus RNA by reverse transcription-polymerase chain reaction in the liver and lymphoid organs but not in the brain in fatal human infection. *Am J Trop Med Hyg* **61**, 720–724.

Schiavetta, A. M., Harre, J. G., Wagner, E., Simmons, M. & Raviprakash, K. (2003). Variable susceptibility of the owl monkey (*Aotus nancymae*) to four serotypes of dengue virus. *Contemp Top Lab Anim Sci* **42**, 12–20.

Shrestha, B., Brien, J. D., Sukupolvi-Petty, S., Austin, S. K., Edeling, M. A., Kim, T., O'Brien, K. M., Nelson, C. A., Johnson, S. & other authors (2010). The development of therapeutic antibodies that neutralize homologous and heterologous genotypes of dengue virus type 1. *PLoS Pathog* **6**, e1000823.

Vaughn, D. W., Green, S., Kalayanarooj, S., Innis, B. L., Nimmannitya, S., Suntayakorn, S., Rothman, A. L., Ennis, F. A. & Nisalak, A. (1997). Dengue in the early febrile phase: viremia and antibody responses. *J Infect Dis* **176**, 322–330.

Whitehead, S. S., Hanley, K. A., Jr, Blaney, J. E., Jr, Gilmore, L. E., Elkins, W. R. & Murphy, B. R. (2003). Substitution of the structural genes of dengue virus type 4 with those of type 2 results in chimeric vaccine candidates which are attenuated for mosquitoes, mice, and rhesus monkeys. *Vaccine* **21**, 4307–4316.

WHO (2002). Dengue and dengue haemorrhagic fever. Fact sheet no. 117.

frontiers in MICROBIOLOGY

ORIGINAL RESEARCH ARTICLE
published: 07 December 2011
doi: 10.3389/fmicb.2011.00240

Long-term persistent GBV-B infection and development of a chronic and progressive hepatitis C-like disease in marmosets

Yuki Iwasaki[1,2†], Ken-ichi Mori[3†], Koji Ishii[4], Noboru Maki[3], Sayuki Iijima[1], Tomoyuki Yoshida[5], Sachi Okabayashi[6], Yuko Katakai[6], Young-Jung Lee[1], Akatsuki Saito[5], Hiromi Fukai[3], Nobuyuki Kimura[1], Naohide Ageyama[1], Sayaka Yoshizaki[4], Tetsuro Suzuki[4], Yasuhiro Yasutomi[1], Tatsuo Miyamura[4], Mari Kannagi[2] and Hirofumi Akari[1,5]*

[1] *Tsukuba Primate Research Center, National Institute of Biomedical Innovation, Tsukuba, Japan*
[2] *Department of Immunotherapeutics, Graduate School of Medicine and Dentistry, Tokyo Medical and Dental University, Tokyo, Japan*
[3] *Advanced Life Science Institute, Wako, Japan*
[4] *Department of Virology II, National Institute of Infectious Diseases, Tokyo, Japan*
[5] *Primate Research Institute, Kyoto University, Inuyama, Japan*
[6] *Corporation for Production and Research of Laboratory Primates, Tsukuba, Japan*

Edited by:
Yasuko Yokota, National Institute of Infectious Diseases, Japan

Reviewed by:
Ikuo Shoji, Kobe University Graduate School of Medicine, Japan
Soon B. Hwang, Hallym University, South Korea

***Correspondence:**
Hirofumi Akari, Primate Research Institute, Kyoto University, Inuyama 484-8506, Japan.
e-mail: akari@pri.kyoto-u.ac.jp

†Yuki Iwasaki and Ken-ichi Mori have contributed equally to this work.

It has been shown that infection of GB virus B (GBV-B), which is closely related to hepatitis C virus, develops acute self-resolving hepatitis in tamarins. In this study we sought to examine longitudinally the dynamics of viral and immunological status following GBV-B infection of marmosets and tamarins. Surprisingly, two of four marmosets but not tamarins experimentally challenged with GBV-B developed long-term chronic infection with fluctuated viremia, recurrent increase of alanine aminotransferase and plateaued titers of the antiviral antibodies, which was comparable to chronic hepatitis C in humans. Moreover, one of the chronically infected marmosets developed an acute exacerbation of chronic hepatitis as revealed by biochemical, histological, and immunopathological analyses. Of note, periodical analyses of the viral genomes in these marmosets indicated frequent and selective non-synonymous mutations, suggesting efficient evasion of the virus from antiviral immune pressure. These results demonstrated for the first time that GBV-B could induce chronic hepatitis C-like disease in marmosets and that the outcome of the viral infection and disease progression may depend on the differences between species and individuals.

Keywords: GBV-B, HCV, marmoset, tamarin, hepatitis C

INTRODUCTION

Among the known viruses, GB virus B (GBV-B) is closely related to hepatitis C virus (HCV), with 25–30% homology at the amino acid level, and is tentatively classified in *Hepacivirus* genus of *Flavivirus* family (Muerhoff et al., 1995; Simons et al., 1995; Ohba et al., 1996). Due to limited epidemiological analyses, the natural host(s) and prevalence of GBV-B have remained to be determined.

Hepatitis C virus is a major causative agent for non-A, non-B hepatitis. HCV is globally disseminated and estimated to be carried by more than 170 million people (Chisari, 2005; Lavanchy, 2009). Most HCV-infected individuals develop chronic liver diseases such as liver cirrhosis and hepatocellular carcinoma (Hoofnagle, 1997; Seeff and Hoofnagle, 2002; Rehermann and Nascimbeni, 2005). Since standard therapy with PEGylated interferon and ribavirin is effective for only about 50% of patients, it is crucial to develop more effective therapeutics (Feld and Hoofnagle, 2005; Melnikova, 2008). The only validated animal model for HCV infection is the chimpanzees. This model has been valuable for determining important aspects of this disease, including the relationship between the virus and the antiviral immune responses of the host and the process of viral pathogenesis (Bukh, 2004; Akari et al., 2009; Boonstra et al., 2009). However, chimpanzees are endangered and present ethical complications and the availability of these experimental animals is severely restricted.

When tamarins (members of the New World monkeys) are infected with GBV-B, they generally develop acute viremia and self-resolving hepatitis as indicated by increases in the levels of serum enzymes such as alanine aminotransferase (ALT) (Bukh et al., 1999; Beames et al., 2000; Beames et al., 2001; Sbardellati et al., 2001; Lanford et al., 2003; Martin et al., 2003; Bright et al., 2004; Jacob et al., 2004; Nam et al., 2004; Kyuregyan et al., 2005; Ishii et al., 2007; Weatherford et al., 2009). Thus, the monkeys have been proposed as a surrogate model of HCV infection of chimpanzee and humans. However, a major hurdle for the development of a monkey-based surrogate model is the difficulties encountered in obtaining chronically infected monkeys that exhibit progression of chronic hepatitis C-like diseases (Martin et al., 2003; Nam et al., 2004; Takikawa et al., 2010).

Abbreviations: ALT, alanine aminotransferase; GBV-B, GB virus B; HCV, hepatitis C virus; HE, hematoxylin and eosin; p.i., post infection.